Published in final edited form as:

Insect Mol Biol. 2018 April ; 27(2): 268–278. doi:10.1111/imb.12370.

Krüppel homolog 1 acts as a repressor and an activator in the transcriptional response to juvenile hormone in adult mosquitoes

Reyhaneh Ojani[*], **Xiaonan Fu**[†], **Tahmina Ahmed**[*], **Pengcheng Liu**[*], and **Jinsong Zhu**[*]

[*]Department of Biochemistry, Virginia Tech, Blacksburg, VA 24061, USA

[†]Program of Genetics, Bioinformatics, and Computational Biology, Virginia Tech, Blacksburg, VA 24061, USA

Abstract

Krüppel homolog 1 (Kr-h1) is a zinc finger transcription factor that is upregulated in insects by juvenile hormone (JH) in metamorphosis and adult reproduction. The molecular function of Kr-h1 in reproduction remains largely unknown. Here we report that AaKr-h1 functions as an important transcription regulator in adult female *Aedes aegypti* mosquitoes. The amount of AaKr-h1 protein increases with rising JH levels after adult emergence, reaches its peak at 48 h after eclosion, then decreases gradually and disappears after blood feeding. RNAi-mediated depletion of AaKr-h1 substantially reduced egg production after blood feeding. Using a chromatin immunoprecipitation (ChIP)-cloning approach, we identified *in vivo* AaKr-h1 binding sites in the previtellogenic female mosquitoes. Binding of AaKr-h1 to the target genes correlated with its protein abundance. Interestingly, RNAi experiments indicated that AaKr-h1 played distinct roles when it bound to individual target genes. For example, depletion of AaKr-h1 led to substantial upregulation of *AAEL005545* and *AAEL004444*, but also significantly decreased the expression of *AAEL005957* and *AAEL013177* when compared with the control mosquitoes. In summary, AaKr-h1 directly binds to the regulatory regions of its target genes and acts as a transcriptional activator or a repressor in a promoter-specific manner.

Keywords

gene regulation; reproduction; RNA interference; chromatin immunoprecipitation

Introduction

The sesquiterpenoid juvenile hormone (JH) is known for its anti-metamorphic action in insects (Nijhout 1994). JH delays metamorphosis of immature larvae until they have reached a proper size and stage. In the last instar larvae, JH decreases to an undetectable level, allowing the molting hormone 20-hydroxyecdysone (20E) to induce metamorphosis (Jindra et al. 2013). JH also plays important roles in the adult stage of insect life. It is involved in

[*]Correspondence: Jinsong Zhu, Department of Biochemistry, Virginia Tech, 340 West Campus Drive, Blacksburg, VA 24061, USA. Tel.: +1 540 231 3841; fax: +1 540 231 9070; zhujin@vt.edu.

many aspects of reproduction, including the previtellogenic development, vitellogenesis, and oogenesis (Raikhel et al. 2005). A critical step in egg production is vitellogenesis, in which the yolk protein precursor vitellogenin (Vg) is synthesized and deposited into developing oocytes. In the yellow fever mosquito, *Aedes aegypti*, JH is required during the previtellogenic phase to make the fat body to become competent for Vg synthesis (Dittmann et al. 1989; Raikhel and Lea 1990). In *Tribolium castaneum*, JH regulates Vg synthesis in the fat body; blocking the JH signaling pathway causes a dramatic decrease in Vg expression and impedes oocyte maturation (Parthasarathy et al. 2010).

The molecular mechanisms underlying JH action have been partially elucidated only in recent years (Jindra et al. 2015). Many of the aforementioned JH functions were mediated by the JH receptor Methoprene-tolerant (MET) (Jindra et al. 2015; Konopova and Jindra 2007). MET is a basic Helix-Loop-Helix/Per-Arnt-Sim (bHLH/PAS) transcription factor (Ashok et al. 1998). In response to JH, MET forms a heterodimer with another bHLH-PAS protein, Taiman (TAI) (Li et al. 2011). The MET-TAI complex recognizes an E-box like sequence (5′-GCACGTG-3′) in the regulatory regions of JH-responsive genes, leading to the transcriptional regulation of these genes (Kayukawa et al. 2012; Li et al. 2014; Zhang et al. 2011).

Another key component in the JH pathway is the Krüppel homolog 1 (Kr-h1) protein. *Kr-h1* is a JH early response gene in many insects and its JH-induced expression relies on the function of MET (Lozano and Belles 2011; Minakuchi et al. 2009; Minakuchi et al. 2008; Zhang et al. 2011; Zhu et al. 2010). Several studies have demonstrated that MET-TAI binds to the juvenile hormone response elements in the promoter of *Kr-h1* and directly regulates its transcription (Cui et al. 2014; Kayukawa et al. 2012; Kayukawa et al. 2013; Li et al. 2014; Shin et al. 2012). *Kr-h1* plays an essential role in the repression of metamorphosis both in holometabolous and hemimetabolous insects (Konopova et al. 2011; Lozano and Belles 2011; Minakuchi et al. 2009; Minakuchi et al. 2008). During the larval stage, JH prevents immature larvae from initiating precocious metamorphosis by suppressing the expression of the pupal specifier Broad-Complex (BR-C) and the adult specifier E93 (Muramatsu et al. 2008; Urena et al. 2014; Zhou et al. 1998; Zhou and Riddiford 2002). Recent studies have demonstrated that this JH-mediated suppression is mediated by Kr-h1 (Kayukawa et al. 2017; Kayukawa et al. 2016; Minakuchi et al. 2009; Minakuchi et al. 2008; Urena et al. 2016).

Kr-h1 contains eight C2H2-type zinc fingers that are highly conserved among insects, and less conserved Glutamine-rich and Proline/Serine/threonine-rich regions at the N- and C-termini, respectively (Konopova et al. 2011; Pecasse et al. 2000). Proteins that contain C2H2-type zinc fingers are primarily transcription factors (Najafabadi et al. 2015). Indeed, a consensus Kr-h1-binding site (KBS) in the promoter regions of *BR-C* and *E93* has been recently identified in a *Bombyx mori* cell line, indicating that Kr-h1 acts as a DNA-binding transcription factor directly repressing the 20E-induced expression of *BR-C* and *E93* (Kayukawa et al. 2017; Kayukawa et al. 2016).

The role of Kr-h1 in female reproduction seems to vary widely among insect species. In the migratory locust *Locusta migratoria*, *Kr-h1* knockdown considerably reduces the JH-

regulated expression of *Vg* and practically blocks oocyte maturation (Song et al. 2014). Depletion of MET and TAI in the linden bug *Pyrrhocoris apterus* suppresses *Vg* expression in the fat body and blocks ovarian development, but knockdown of *Kr-h1* does not cause an evident phenotypic change during vitellogenesis (Smykal et al. 2014). In the common bed bug, *Cimex lectularius*, *Kr-h1* knockdown in adult females does not reduce the number of eggs oviposited but severely affects the hatching of those eggs (Gujar and Palli 2016). In adult female *Ae. aegypti* mosquitoes, JH regulates the expression of a large number of genes during the post-emergence development (Zou et al. 2013). The role played by the mosquito Kr-h1 in this JH action is not well understood. Here we reported our identification of the Kr-h1 target genes in adult *Ae. aegypti*. Using chromatin immunoprecipitation, we cloned a number of *in vivo* binding sites of AaKr-h1. Maximal binding of AaKr-h1 to those locations took place at 48 h post-eclosion, approximately coincident with the peak of the AaKr-h1 protein levels. RNAi experiments showed that AaKr-h1 functioned as a transcription factor, regulating the expression of its direct target genes and playing an essential role in egg production. Interestingly, depletion of AaKr-h1 caused opposing effects on the expression of individual target genes in the fat body, suggesting that AaKr-h1 can both activate and repress gene expression in response to JH.

Results

Expression of AaKr-h1 in the fat body of adult female *Ae. aegypti* mosquitoes

Fat bodies were collected from adult female mosquitoes at 0 h, 12 h, 24 h, 36 h, 48 h, 96 h post-eclosion (PE) and also at 12 h post blood meal (PBM). The mRNA levels of *AaKr-h1* were measured with quantitative real-time polymerase chain reactions (qRT-PCR). Our previous study has demonstrated that AaKr-h1 is upregulated by JH in the newly emerged mosquitoes (Zhu et al., 2010). As expected, the mRNA level of *AaKr-h1* rose gradually after eclosion and increased 2.8 fold ($p<0.01$) to the highest level at 48 h PE (Figure 1A). After blood ingestion, the expression of *AaKr-h1* decreased dramatically; the amount of AaKr-h1 mRNA at 12 h PBM was lower than that at eclosion (Figure 1A).

The protein levels of AaKr-h1 were also examined in the fat body of the adult female mosquitoes. AaKr-h1, undetectable in the mosquitoes at 0 h and 12 h PE, became evident at 24 h PE (Figure 1B). The protein levels continued to increase, peaked at 48 h PE, and then decreased considerably at 96 h PE. At 12 h after a blood meal, AaKr-h1 was undetectable again (Figure 1B). The expression of AaKr-h1 correlated well with the JH titers in female mosquitoes.

AaKr-h1 is required for egg production in *Ae. aegypti* mosquitoes

To examine the role of AaKr-h1 in egg production, the expression of *AaKr-h1* in *Ae. aegypti* was knocked down using RNAi. Newly emerged adult female mosquitoes were injected with dsRNA for AaKr-h1 or green fluorescent protein (GFP). The successful knockdown of AaKr-h1 was confirmed by quantitative RT-PCR and Western Blot analysis (Figure 2). While the previtellogenic growth of primary follicles is known to be controlled by JH, the knockdown of AaKr-h1 did not significantly affect the growth (Figure 2C). Five days after injection, the un-injected, dsGFP-injected, and dsKr-h1-injected mosquitoes were blood-fed

on anesthetized mice. The number of eggs laid by each female mosquito was counted manually and the data were analyzed using GraphPad software (Figure 2B). The results indicated that the dsKr-h1-injected mosquitoes produced 46% fewer eggs compared with the dsGFP-injected ones ($p<0.001$). However, there was no significant difference in the number of eggs between the un-injected and dsGFP-injected controls ($p>0.1$). These results indicated that AaKr-h1 plays an important role in the JH-regulated mosquito reproduction.

Identification of the AaKr-h1 target genes in adult mosquitoes

To find genes that are directly regulated by AaKr-h1 in the previtellogenic stage, a chromatin immunoprecipitation (ChIP) experiment was performed to clone the *in vivo* DNA binding sites of AaKr-h1 in mosquitoes. Mosquito abdomens were collected from female adults at 48 h PE. The samples were treated with formaldehyde to covalently stabilize protein-DNA complexes. After chromatin was fragmented by nuclease digestion, the specific antibody of AaKr-h1 was used to capture this protein with its associated genomic DNA. The DNA fragments were then purified and cloned into a TOPO cloning vector. Several hundred colonies were obtained after bacterial transformation; plasmid DNA was purified from 60 randomly picked clones for DNA sequencing. Bioinformatic analysis was performed using the *Ae. aegypti* genome database to localize the DNA fragments associated with AaKr-h1. After mapping an AaKr-h1-binding sequence to the *Ae. aegypti* genome, the nearest gene to that sequence was considered as an AaKr-h1 target gene. The identified AaKr-h1-binding regions and their putatively associated genes are listed in Table 1.

To verify that the cloned DNA sequences were indeed bound by AaKr-h1 *in vivo*, standard ChIP experiments were performed using the abdomens of female mosquitoes collected at 48 h PE. The ChIP assays were carried out in parallel with the AaKr-h1 antibody and the nonspecific rabbit IgG. Enrichment of four identified AaKr-h1 DNA-binding sites (regulatory regions of *AAEL000741*, *AAEL003050*, *AAEL005651,* and *AAEL005957*) was compared between the DNA precipitated by the AaKr-h1 antibody and the rabbit IgG. Significant higher enrichment ($p<0.01$) was observed for all four binding sites when ChIP was performed with the AaKr-h1 antibody (Figure 3A). In the DNA enriched by the AaKr-h1 antibody, we further compared the binding of AaKr-h1 to different regions of the mosquito gene *AAEL005957*. The binding of AaKr-h1 to the identified 5′ regulatory region was 8.1-fold stronger than to a downstream control region ($p<0.05$) (Figure 3B). These experiments suggested that the identified DNA sequences are the specific DNA binding sites of AaKr-h1 in the previtellogenic mosquitoes.

A total of 39 AaKr-h1-binding sites were detected at 48 h PE within 100 kb of well-annotated genes. Some of the binding sites were only several hundred base pairs upstream of the putative transcriptional start sites. Sequences homologous to the core KBS of *BmBR-C* were discovered in the 39 AaKr-h1 binding sites (Supplementary Figure 2). Among the 39 AaKr-h1 target genes, 21 genes had unknown functions. The other 18 genes were assigned with various functions: metabolism (15.4%), cellular processes and signaling (20.5%), and information storage and processing (10.3%) (Supplementary Figure 1). Among the target genes, *AAEL005810*, *AAEL013177, AAEL005957, AAEL014226*, *AAEL004444,* and *AAEL005545,* have been previously reported to be under the control of AaMET (Zou et al.,

2013). The first three genes (*AAEL005810*, *AAEL013177,* and *AAEL005957*) were downregulated in the newly emerged mosquitoes when AaMET was knocked down by RNAi, while the latter three were upregulated in the AaMET RNAi mosquitoes (Zou et al. 2013).

The DNA binding patterns of AaKr-h1 on individual target genes

The dynamics of AaKr-h1 binding to the six genes (*AAEL005810*, *AAEL013177, AAEL005957, AAEL014226*, *AAEL004444,* and *AAEL005545*) was investigated in female mosquitoes at 0 h, 12 h, 24 h, 36 h, 48 h, 96 h post eclosion and at 12 h post blood meal. ChIP experiments were performed using the AaKr-h1 antibody, and rabbit IgG was used as a control. The *in vivo* binding of AaKr-h1 to the identified regulatory regions of all six genes increased after eclosion and reached to the highest level within 48 h PE (Figure 4). Also, for all the examined sequences, the binding of AaKr-h1 decreased considerably at 96 h PE and dropped further to the lowest level at 12 h PBM (Figure 4). These results suggested that the *in vivo* binding of AaKr-h1 to its target genes depends on its protein abundance (Figure 1).

Knockdown of *AaKr-h1* has opposing effects on individual AaKr-h1 target genes

While AaKr-h1 bound to the abovementioned six genes in a similar manner in the previtellogenic stage, expression of those genes displayed two distinct patterns. The mRNA levels of *AAEL005810*, *AAEL013177,* and *AAEL005957* increased by 1.8–2.5 fold after eclosion and peaked at 48 h PE. The mRNAs then decreased gradually and dropped to the lowest levels at 12 h PBM (Figure 5A). The expression profiles of these three genes correlated well with the mRNA profile of *AaKr-h1* (Figure 1A). To investigate how AaKr-h1 regulates the transcription of these genes, newly emerged female *Ae. aegypti* mosquitoes were injected with dsRNA for *AaKr-h1* or *GFP*. At 96 h PE, the knockdown of *AaKr-h1* was verified in the fat body of the *AaKr-h1 RNAi* mosquitoes (Supplementary Figure 3). The RNAi-mediated depletion of AaKr-h1 decreased the expression of *AAEL005810*, *AAEL013177* and *AAEL005957* by 2.9, 1.8 and 1.9 fold ($p<0.05$), respectively, compared to the dsGFP-injected mosquitoes (Figure 5B). However, the dsGFP injection did not show any significant effect on the expression of these genes ($p>0.1$). This result indicated that AaKr-h1 functions as a transcriptional activator for *AAEL005810*, *AAEL013177* and *AAEL005957*.

On the other hand, the expression of *AAEL014226*, *AAEL004444*, and *AAEL005545* showed a different pattern when they were compared with the mRNA profile of *AaKr-h1*. Their mRNA levels generally decreased after adult emergence, dropped to the lowest amounts at 48 h PE, and then gradually went up after that (Figure 6A). The lowest expression at 48 h PE coincided with the maximal binding of AaKr-h1 to the target sites in the regulatory regions of *AAEL014226*, *AAEL004444*, and *AAEL005545* (Figure 4). The knockdown of *AaKr-h1* increased the expression of *AAEL014226*, *AAEL004444* and *AAEL005545* at 96 h PE by 2.0, 2.6 and 1.6 fold, respectively, compared with the dsGFP - injected control (Figure 6B). This observation implied that AaKr-h1 acted as a transcriptional repressor of *AAEL014226*, *AAEL004444,* and *AAEL005545*. These data suggested that AaKr-h1 exerts gene-specific roles in transcription activation and repression; it positively regulates some target genes and negatively regulates other target genes.

Discussion

MET has been shown to regulate a large number of genes in adult mosquitoes in response to JH (Zou et al. 2013). The early response genes, which include genes encoding transcription factors such as Kr-h1 and Hairy, are controlled directly by MET. MET may regulate many other genes indirectly via the action of the early gene products. Indeed, Hairy has been reported to mediate the action of MET in gene repression (Saha et al. 2016). The Hairy target genes identified in the fat body of female *Ae. aegypti* mosquitoes overlapped substantially with the JH-repressed genes identified by the depletion of MET (Saha et al. 2016). The evidence presented in our current study clearly indicates that Kr-h1 is a key intermediate player in the JH signaling pathway. Using the ChIP-cloning strategy, we identified a small group of mosquito genes that were directly bound and transcriptionally regulated by AaKr-h1 in the previtellogenic mosquitoes. These genes represented a diverse array of functions. Knockdown of *AaKr-h1* in adult female mosquitoes considerably reduced their fecundity.

In the fat body of previtellogenic female mosquitoes, AaKr-h1 acted as a bifunctional transcription factor capable of activating or repressing transcription. Kr-h1 contains a cluster of eight zinc fingers. Tandem modular C2H2 zinc finger domains each contact three or more nucleotides. It is possible not all of the eight domains engage DNA simultaneously. The multiple zinc fingers provide the potential to recognize very diverse DNA sequences. Binding to different sequences may force Kr-h1 to adopt different conformations that lead to recruitment of coactivator or corepressor proteins. Therefore, Kr-h1 can exert opposing effects on different promoters. To test this hypothesis, it is imperative to separate the Kr-h1 target genes that are upregulated by Kr-h1 from those that are downregulated by Kr-h1. Alignment of the Kr-h1 binding sites from each gene group would yield consensus motifs for comparison. A comprehensive ChIP-seq analysis and an RNA-seq analysis of the *AaKr-h1 RNAi* mosquitoes are currently underway to address this question.

In addition to their function in DNA binding, the C2H2 zinc finger domains are also involved in many protein-protein interactions (Brayer and Segal 2008). Although Kr-h1 seems to be capable of binding to KBS all by itself (Kayukawa et al. 2017; Kayukawa et al. 2016), other transcription factors could possibly bind to the vicinity of the Kr-h1 binding sites, interacting with Kr-h1 and modulating the transactivation activity of Kr-h1. Since MET and Hairy are also important transcriptional regulators mediating the JH action, more studies are needed in the future to investigate whether these two proteins and Kr-h1 are loaded on the same JH-regulated promoters, collaboratively modulating the gene transcription.

The transactivation activity of Kr-h1 may also be converted by posttranslational modifications. We have reported that JH activates the phospholipase C (PLC) pathway in *Ae. aegypti* mosquitoes and subsequently activates calcium/calmodulin-dependent protein kinase II (CaMKII) and protein kinase C (PKC) (Liu et al. 2015; Ojani et al. 2016). It is conceivable that Kr-h1 serves as the direct or indirect target of CaMKII or PKC, and that phosphorylation modification switches its function between an activator and a repressor. However, this can’t explain how Kr-h1 exerts opposing effects on individual genes as all the

Kr-h1 proteins should be posttranslationally modified in the same fashion in the fat body at the same developmental stage.

Among the genes that were occupied by AaKr-h1 at 48 h PE is *E74*, a 20E early response gene. *E74* is not expressed in the previtellogenic stage because the 20E concentrations increase only after a blood meal. Binding of AaKr-h1 to the *E74* gene may either preclude the expression of *E74* before blood feeding or keep this gene in a poised state for later activation. In *Drosophila*, Kr-h1 was first identified as a stage-specific modulator of the prepupal ecdysone response (Pecasse et al. 2000). In the homozygous *Kr-h1* mutant, several key genes of the ecdysone regulatory hierarchies display a shift in their time of expression in salivary glands (Pecasse et al. 2000). We are currently testing whether AaKr-h1 has a similar role in modulating the vitellogenic 20E response in adult mosquitoes.

Experimental procedures

Mosquito rearing

Ae. aegypti mosquitoes of the Liverpool strain were maintained at 28°C and 60–70% humidity, with a 14/10 h day/night light cycle. Mosquito larvae were fed on pulverized fish food (TetraMin Tropical Flakes) and adults were provided with a 10% sucrose solution. Female mosquitoes (7 days post-eclosion) were fed on anesthetized mice to stimulate egg production.

Expression and purification of recombinant AaKr-h1

The codon usage of *AaKr-h1* cDNA was optimized for bacterial expression. The optimized cDNA for the N-terminal (amino acid residues 1–461) and C-terminal (amino acid residues 363–702) AaKr-h1 was cloned separately into the expression vector pGEX-6P-1 (GE healthcare) between BamHI and XhoI restriction sites (Supplementary Table 1), resulting in the following expression plasmids: NKrh-pGEX-6P-1 and CKrh-pGEX-6P-1.

The plasmids were individually transformed into *Escherichia coli* BL21(DE3). The cells were cultured in Luria-Bertani (LB) medium at 37°C to reach an OD600 of 0.8. After that isopropyl β-D-1-thiogalactopyranoside (IPTG) was added to the media to a final concentration of 0.1 mM and the cultures were grown at 28°C for six more hours. The cell pellet was re-suspended in lysis buffer [150 mM NaCl, 20 mM sodium phosphate, pH 7.3, 2 mM DTT, 1 mM PMSF, 1× Halt protease inhibitor (Thermo Scientific)]. DeBEE high-pressure homogenizer (BEE international) was used to lyse the cells. Affinity purification was carried out using ÄKTA prime and GSTrap FF columns (GE Healthcare). The buffers used for this protein purification were: binding buffer (20 mM sodium phosphate, pH 7.3, 150 mM NaCl, 2 mM DTT) and elution buffer (50 mM Tris-HCl, pH 8, 10 mM reduced glutathione, 2 mM DTT). Purified proteins were dialyzed in PBS buffer and then concentrated using Pierce concentrators.

One milligram each of GST-NKr-h1 and GST-CKr-h1 was combined and sent to Thermo Scientific for antibody production in rabbits. Polyclonal antibodies were affinity purified from the rabbit antisera using the antigens immobilized on Aminolink plus coupling resin (Thermo Scientific), according to the manufacturer's instruction.

Western blot analysis

Whole cell lysates were extracted from fat bodies using a modified RIPA buffer (20 mM Tris-HCl, pH 7.5, 150 mM NaCl, 1 mM EDTA, 1% Triton X-100, 0.1% SDS, 1% sodium deoxycholate, 2.5 mM sodium pyrophosphate, 1 mM sodium orthovanadate, and 1 mM sodium fluoride). Protein concentrations were measured using the bicinchoninic acid (BCA) assay. An equal amount of protein was loaded into each lane and separated on an SDS-PAGE gel in all experiments. Anti-GAPDH antibody (Thermo Scientific) was used at 1:5000 dilution as a loading control for immunoblotting.

Chromatin immunoprecipitation

Abdomens were collected from 100 adult female mosquitoes for each ChIP-cloning experiment. The ChIP assay was performed using the SimpleChIP Plus Enzymatic Chromatin Immunoprecipitation Kit (Cell Signaling Technology) according to the manufacturer's instruction. Briefly, the tissues were grounded in liquid nitrogen and were then homogenized in PBS on ice. Formaldehyde was added to a final concentration of 1%, and crosslinking was performed for 10 minutes at 37°C. Crosslinking was stopped by adding 1.25 M glycine to reach a final concentration of 125 mM. After nuclei preparation, chromatin digestion was performed using 0.25 μl of Micrococcal nuclease for 5 min at 37°C. Immunoprecipitation was carried out using the purified AaKr-h1 antibody. Nonspecific rabbit IgG was used as a negative control.

Cloning of the AaKr-h1-binding sites

DNA purified from the ChIP assays was treated with T4 DNA ligase (New England Biolabs) to make blunt ends. Briefly, 2.5 μg of DNA and 0.75 μl of T4 DNA ligase enzyme were incubated for 15 minutes at 12°C. To stop the reaction, 10 mM EDTA was added to the tube and incubated for 20 minutes at 75°C. The DNA fragments were cleaned using a QIAGEN mini-elute column and cloned into pCR4-TOPO (Life Technology). Competent *E. coli* cells were transformed by the DNA library and were selected on LB agar plates supplemented with kanamycin. Plasmid DNA from sixty randomly picked clones was isolated and sequenced. The DNA sequences were mapped to the *Aedes aegypti* genome.

Quantitative RT-PCR analysis

Total RNA was extracted from mosquito tissues using TRIzol reagent (Life Technologies). The first strand cDNA was synthesized using oligo (dT) primer and the Maxima First Strand cDNA Synthesis Kit (Thermo Scientific). Quantitative PCR was performed in triplicate on an ABI 7300 system (Applied Biosystem) using the GoTaq qPCR Master Mix (Promega). Transcript abundance was normalized to that of rpS7 and analyzed by the Student's t-test for significance. The primers used in qRT-PCR are listed in Supplementary Table 2.

Double-stranded RNA (dsRNA)-induced gene silencing

DsRNAs were synthesized by *in vitro* transcription of a PCR-generated DNA template containing the T7 promoter sequence on both ends (Supplementary Table 3). Female mosquitoes were injected with 0.5 μg of dsRNA within 30 min after eclosion. DsRNA for green fluorescent protein (GFP) was used as a negative control. Four days after dsRNA

injection, RNA was extracted from the injected mosquitoes and the expression of selected genes was analyzed by real-time PCR.

Supplementary Material

Refer to Web version on PubMed Central for supplementary material.

Acknowledgments

This work was supported by NIH grant R01 AI099250 to JZ. Funding for this work was provided in part, by the Virginia Agricultural Experiment Station and the Hatch Program (Accession Number: 1005118) of the National Institute of Food and Agriculture, U.S. Department of Agriculture.

References

Ashok M, Turner C, Wilson TG. Insect juvenile hormone resistance gene homology with the bHLH-PAS family of transcriptional regulators. Proc Natl Acad Sci USA. 1998; 95:2761–2766. [PubMed: 9501163]

Brayer KJ, Segal DJ. Keep your fingers off my DNA: protein-protein interactions mediated by C2H2 zinc finger domains. Cell Biochem Biophys. 2008; 50:111–31. [PubMed: 18253864]

Cui Y, Sui Y, Xu J, Zhu F, Palli SR. Juvenile hormone regulates Aedes aegypti Kruppel homolog 1 through a conserved E box motif. Insect Biochem Mol Biol. 2014; 52:23–32. [PubMed: 24931431]

Dittmann F, Kogan PH, Hagedorn HH. Ploidy levels and DNA-synthesis in fat body cells of the adult mosquito, Aedes aegypti - the role of juvenile hormone. Archives of Insect Biochemistry and Physiology. 1989; 12:133–143.

Gujar H, Palli SR. Juvenile hormone regulation of female reproduction in the common bed bug, Cimex lectularius. Sci Rep. 2016; 6:35546. [PubMed: 27762340]

Jindra M, Belles X, Shinoda T. Molecular basis of juvenile hormone signaling. Curr Opin Insect Sci. 2015; 11:39–46. [PubMed: 28285758]

Jindra M, Palli SR, Riddiford LM. The juvenile hormone signaling pathway in insect development. Annu Rev Entomol. 2013; 58:181–204. [PubMed: 22994547]

Kayukawa T, Jouraku A, Ito Y, Shinoda T. Molecular mechanism underlying juvenile hormone-mediated repression of precocious larval-adult metamorphosis. Proc Natl Acad Sci U S A. 2017; 114:1057–1062. [PubMed: 28096379]

Kayukawa T, Minakuchi C, Namiki T, Togawa T, Yoshiyama M, Kamimura M, Mita K, Imanishi S, Kiuchi M, Ishikawa Y, Shinoda T. Transcriptional regulation of juvenile hormone-mediated induction of Kruppel homolog 1, a repressor of insect metamorphosis. Proc Natl Acad Sci U S A. 2012; 109:11729–34. [PubMed: 22753472]

Kayukawa T, Nagamine K, Ito Y, Nishita Y, Ishikawa Y, Shinoda T. Kruppel Homolog 1 Inhibits Insect Metamorphosis via Direct Transcriptional Repression of Broad-Complex, a Pupal Specifier Gene. J Biol Chem. 2016; 291:1751–62. [PubMed: 26518872]

Kayukawa T, Tateishi K, Shinoda T. Establishment of a versatile cell line for juvenile hormone signaling analysis in Tribolium castaneum. Sci Rep. 2013; 3:1570. [PubMed: 23535851]

Konopova B, Jindra M. Juvenile hormone resistance gene Methoprene-tolerant controls entry into metamorphosis in the beetle Tribolium castaneum. Proc Natl Acad Sci U S A. 2007; 104:10488–93. [PubMed: 17537916]

Konopova B, Smykal V, Jindra M. Common and distinct roles of juvenile hormone signaling genes in metamorphosis of holometabolous and hemimetabolous insects. PLoS One. 2011; 6:e28728. [PubMed: 22174880]

Li M, Liu P, Wiley JD, Ojani R, Bevan DR, Li J, Zhu J. A steroid receptor coactivator acts as the DNA-binding partner of the methoprene-tolerant protein in regulating juvenile hormone response genes. Mol Cell Endocrinol. 2014; 394:47–58. [PubMed: 25004255]

Li M, Mead EA, Zhu J. Heterodimer of two bHLH-PAS proteins mediates juvenile hormone-induced gene expression. Proc Natl Acad Sci U S A. 2011; 108:638–43. [PubMed: 21187375]

Liu P, Peng HJ, Zhu J. Juvenile hormone-activated phospholipase C pathway enhances transcriptional activation by the methoprene-tolerant protein. Proc Natl Acad Sci U S A. 2015; 112:E1871–9. [PubMed: 25825754]

Lozano J, Belles X. Conserved repressive function of Kruppel homolog 1 on insect metamorphosis in hemimetabolous and holometabolous species. Sci Rep. 2011; 1:163. [PubMed: 22355678]

Minakuchi C, Namiki T, Shinoda T. Kruppel homolog 1, an early juvenile hormone-response gene downstream of Methoprene-tolerant, mediates its anti-metamorphic action in the red flour beetle Tribolium castaneum. Dev Biol. 2009; 325:341–50. [PubMed: 19013451]

Minakuchi C, Zhou X, Riddiford LM. Kruppel homolog 1 (Kr-h1) mediates juvenile hormone action during metamorphosis of Drosophila melanogaster. Mech Dev. 2008; 125:91–105. [PubMed: 18036785]

Muramatsu D, Kinjoh T, Shinoda T, Hiruma K. The role of 20-hydroxyecdysone and juvenile hormone in pupal commitment of the epidermis of the silkworm, Bombyx mori. Mech Dev. 2008; 125:411–20. [PubMed: 18331786]

Najafabadi HS, Mnaimneh S, Schmitges FW, Garton M, Lam KN, Yang A, Albu M, Weirauch MT, Radovani E, Kim PM, Greenblatt J, Frey BJ, Hughes TR. C2H2 zinc finger proteins greatly expand the human regulatory lexicon. Nat Biotechnol. 2015; 33:555–62. [PubMed: 25690854]

Nijhout, HF. Insect Hormones. Princeton University Press; 1994.

Ojani R, Liu P, Fu X, Zhu J. Protein kinase C modulates transcriptional activation by the juvenile hormone receptor methoprene-tolerant. Insect Biochem Mol Biol. 2016; 70:44–52. [PubMed: 26689644]

Parthasarathy R, Sun Z, Bai H, Palli SR. Juvenile hormone regulation of vitellogenin synthesis in the red flour beetle, Tribolium castaneum. Insect Biochem Mol Biol. 2010; 40:405–14. [PubMed: 20381616]

Pecasse F, Beck Y, Ruiz C, Richards G. Kruppel-homolog, a stage-specific modulator of the prepupal ecdysone response, is essential for Drosophila metamorphosis. Dev Biol. 2000; 221:53–67. [PubMed: 10772791]

Raikhel, A., Brown, M., Belles, X. Hormonal control of reproductive processes. In: Gilbert, L.Iatrou, K., Gill, SS., editors. Comprehensive Molecular Insect Science. Vol. 3. Elsevier; Pergamon: 2005. p. 433-491.Endocrinology

Raikhel AS, Lea AO. Juvenile hormone controls previtellogenic proliferation of ribosomal RNA in the mosquito fat body. General and Comparative Endocrinology. 1990; 77:423–434. [PubMed: 1970970]

Saha TT, Shin SW, Dou W, Roy S, Zhao B, Hou Y, Wang XL, Zou Z, Girke T, Raikhel AS. Hairy and Groucho mediate the action of juvenile hormone receptor Methoprene-tolerant in gene repression. Proc Natl Acad Sci U S A. 2016; 113:E735–43. [PubMed: 26744312]

Shin SW, Zou Z, Saha TT, Raikhel AS. bHLH-PAS heterodimer of methoprene-tolerant and Cycle mediates circadian expression of juvenile hormone-induced mosquito genes. Proc Natl Acad Sci U S A. 2012; 109:16576–81. [PubMed: 23012454]

Smykal V, Bajgar A, Provaznik J, Fexova S, Buricova M, Takaki K, Hodkova M, Jindra M, Dolezel D. Juvenile hormone signaling during reproduction and development of the linden bug, Pyrrhocoris apterus. Insect Biochem Mol Biol. 2014; 45:69–76. [PubMed: 24361539]

Song J, Wu Z, Wang Z, Deng S, Zhou S. Kruppel-homolog 1 mediates juvenile hormone action to promote vitellogenesis and oocyte maturation in the migratory locust. Insect Biochem Mol Biol. 2014; 52:94–101. [PubMed: 25017142]

Urena E, Chafino S, Manjon C, Franch-Marro X, Martin D. The Occurrence of the Holometabolous Pupal Stage Requires the Interaction between E93, Kruppel-Homolog 1 and Broad-Complex. PLoS Genet. 2016; 12:e1006020. [PubMed: 27135810]

Urena E, Manjon C, Franch-Marro X, Martin D. Transcription factor E93 specifies adult metamorphosis in hemimetabolous and holometabolous insects. Proc Natl Acad Sci U S A. 2014; 111:7024–9. [PubMed: 24778249]

Zhang Z, Xu J, Sheng Z, Sui Y, Palli SR. Steroid receptor co-activator is required for juvenile hormone signal transduction through a bHLH-PAS transcription factor, methoprene tolerant. J Biol Chem. 2011; 286:8437–47. [PubMed: 21190938]

Zhou B, Hiruma K, Shinoda T, Riddiford LM. Juvenile hormone prevents ecdysteroid-induced expression of broad complex RNAs in the epidermis of the tobacco hornworm, Manduca sexta. Dev Biol. 1998; 203:233–44. [PubMed: 9808776]

Zhou X, Riddiford LM. Broad specifies pupal development and mediates the 'status quo' action of juvenile hormone on the pupal-adult transformation in Drosophila and Manduca. Development. 2002; 129:2259–69. [PubMed: 11959833]

Zhu J, Busche JM, Zhang X. Identification of juvenile hormone target genes in the adult female mosquitoes. Insect Biochem Mol Biol. 2010; 40:23–9. [PubMed: 20018242]

Zou Z, Saha TT, Roy S, Shin SW, Backman TW, Girke T, White KP, Raikhel AS. Juvenile hormone and its receptor, methoprene-tolerant, control the dynamics of mosquito gene expression. Proc Natl Acad Sci U S A. 2013; 110:E2173–81. [PubMed: 23633570]

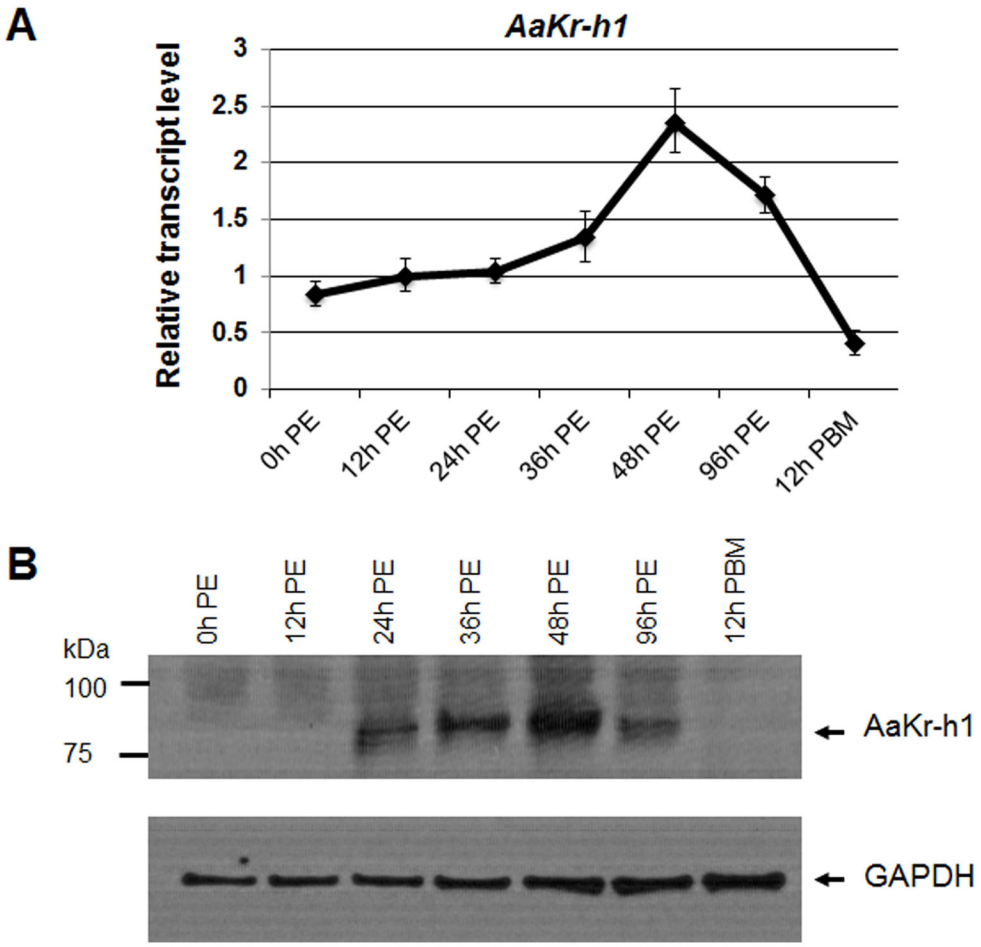

Figure 1.

Expression profile of *AaKr-h1* in the fat body of previtellogenic female mosquitoes. (*A*) Adult female mosquitoes were collected at the indicated time points. The mRNA of *AaKr-h1* was measured using real-time PCR. Results are the mean ± S.D. of three replicates. PE, post eclosion; PBM, post blood meal. (*B*) Protein profile of AaKr-h1 in female *Ae. aegypti* mosquitoes. Western blot analysis was conducted using the AaKr-h1 antibody. The GAPDH antibody was used for the loading control.

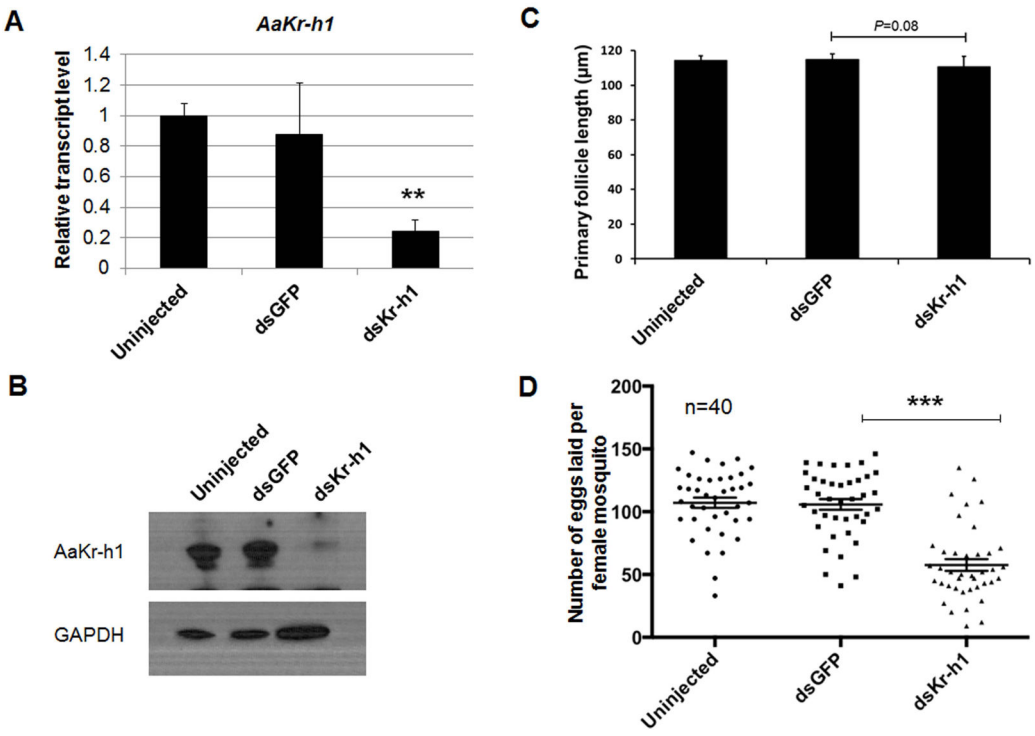

Figure 2.

RNAi-mediated knockdown of *AaKr-h1* reduced egg production in *Ae. aegypti* mosquitoes. (*A*) The expression of *AaKr-h1* was successfully knocked down in the *dsKr-h1* injected mosquitoes. Newly emerged adult female mosquitoes were injected with dsRNAs for *AaKr-h1* or *GFP* (as control). A group of three mosquitoes was randomly picked from the un-injected, *dsGFP*- and *dsKr-h1*-injected mosquitoes at 96 h PE. The mRNA levels of *AaKr-h1* were measured by real-time PCR. Results are the mean ± S.D. of three replicates. Statistical analysis was conducted by a paired t-test (**, $p<0.01$). (*B*) Knockdown of *AaKr-h1* was confirmed by Western Blot. Proteins were extracted from the un-injected, *dsGFP*- and *dsKr-h1*-injected mosquitoes at 96 h PE. Western Blot analysis was conducted using anti-AaKr-h1 antibody. Anti-GAPDH antibody was used for the loading control. (*C*) Effect of the *AaKr-h1* knockdown on the previtellogenic growth of primary follicles. Follicle lengths were measured at 96 h PE. Each bar represents mean ± S.D. of five independent measurements of follicles from ten mosquitoes in each group. Statistical analysis was conducted by a paired t-test. (*D*) Egg production after blood feeding in the *AaKr-h1 RNAi* mosquitoes. Dots represent egg counts for individual mosquitoes within 5 days after the blood meal. Lines represent mean numbers of eggs oviposited from three replicates; bars indicate the standard error of the mean (SEM). Data were analyzed using GraphPad software. Statistical analysis was conducted using a paired t-test (***, $p<0.001$).

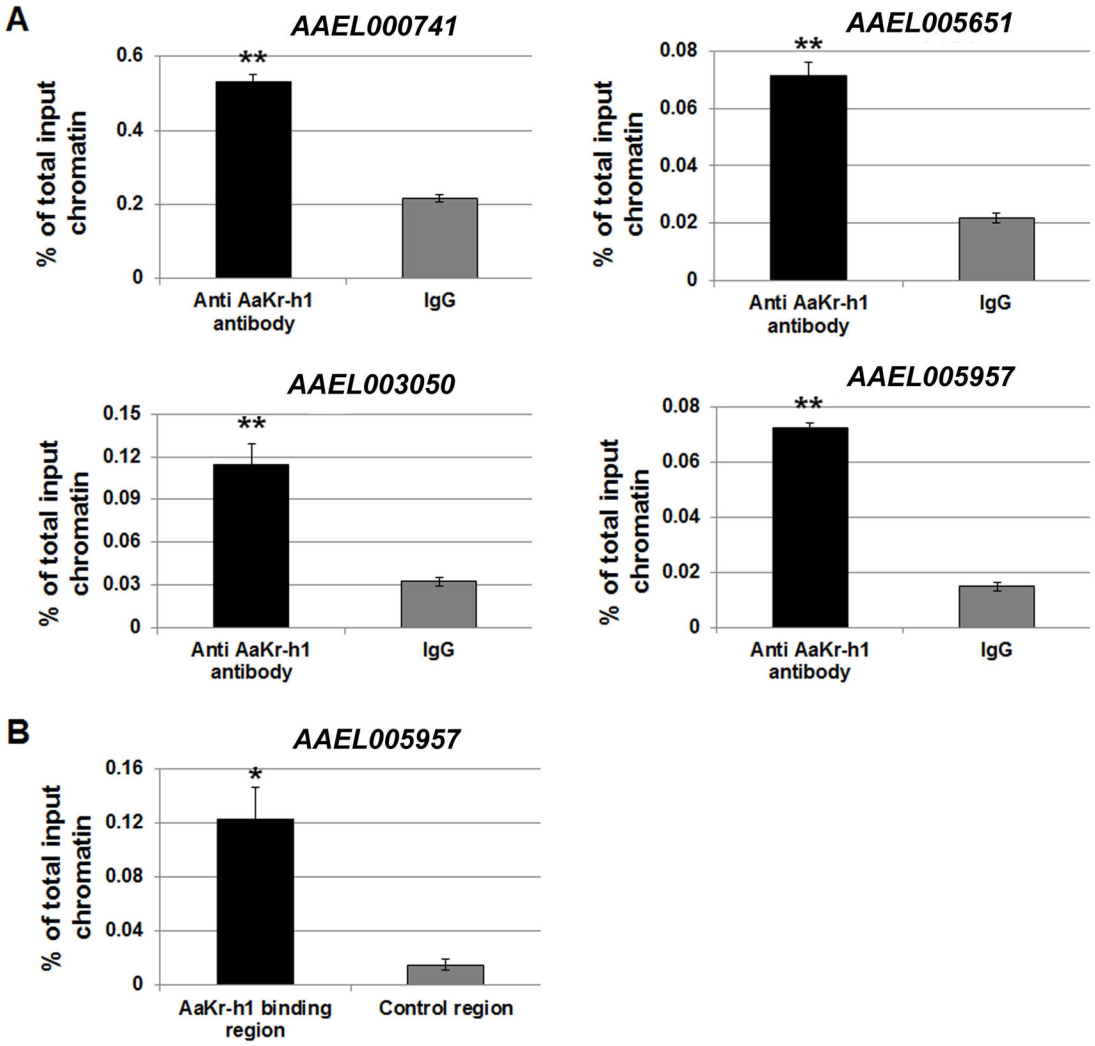

Figure 3.

Verification of the *in vivo* binding of AaKr-h1 to the DNA sequences that were identified by ChIP-cloning. (*A*) Enrichment of four sequences was confirmed in an independent ChIP assay using mosquito abdomens collected at 48 h PE. The AaKr-h1 antibody and rabbit IgG (as control) were used in this ChIP experiment. Real-time PCR was performed to compare the enrichment of the AaKr-h1 binding sequences between the immunoprecipitations with the AaKr-h1 antibody and with rabbit IgG. (*B*) Selective binding of AaKr-h1 to the regulatory region of *AAEL005957*. After chromatin immunoprecipitation with the AaKr-h1 antibody, the precipitated DNA was analyzed using real-time PCR to compare the enrichment of the regulatory region identified by ChIP-cloning and a control region in the coding sequence of *AAEL005957*. Results are shown as a percentage of input chromatin and represent mean value ± S.D. of three replicates. Statistical analysis was conducted using a paired t-test (**, $p<0.01$; *, $p<0.05$).

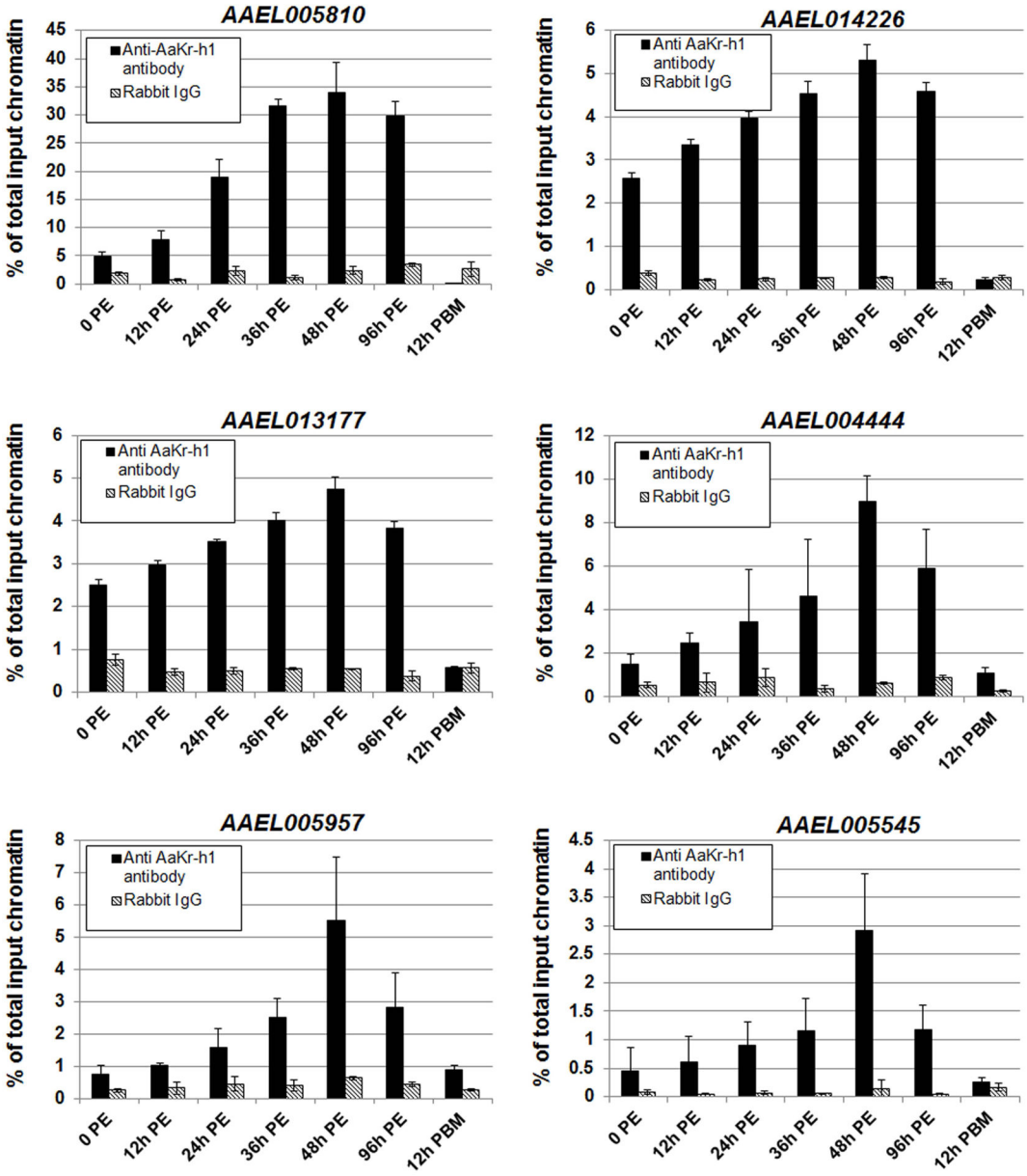

Figure 4.

Binding of AaKr-h1 to the regulatory regions of individual AaKr-h1 target genes. Abdomens of 100 female mosquitoes were collected at the indicated time points. The ChIP experiments were performed using the ant-AaKr-h1 antibody and non-specific rabbit IgG (as control). After chromatin immunoprecipitation, the enrichment of the relevant AaKr-h1 binding sequence was determined using real-time PCR. Results are shown as a percentage of input chromatin and represent mean value ± S.D. of three replicates.

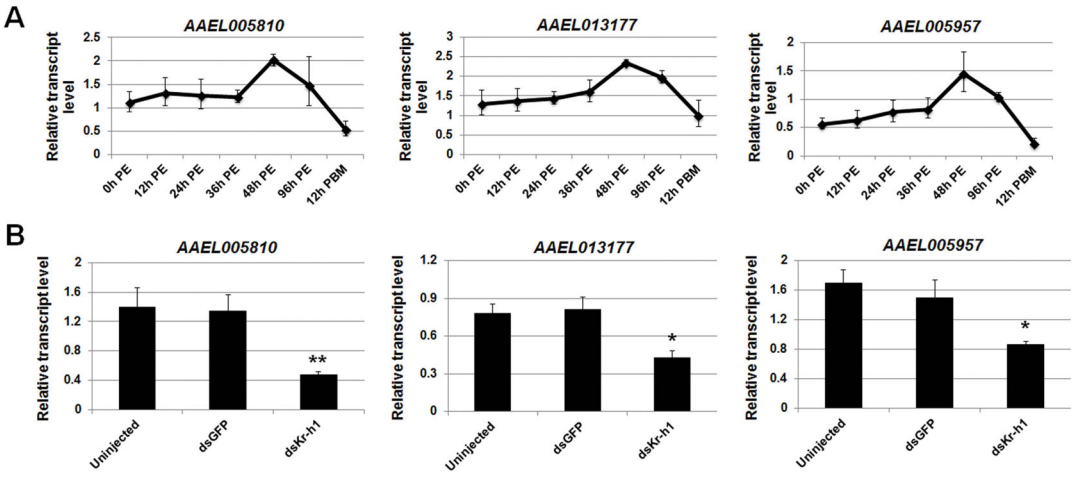

Figure 5.

RNAi-mediated knockdown of *AaKr-h1* led to the downregulation of *AAEL005810*, *AAEL013177,* and *AAEL005957*. (*A*) The mRNA profiles of these three AaKr-h1 target genes in the fat body of previtellogenic female mosquitoes. Total RNA was extracted and the expression of AaKr-h1 target genes was measured using real-time PCR. (*B*) Expression of the AaKr-h1 target genes in the AaKr-h1-depleted mosquitoes. Newly emerged female mosquitoes were injected with dsRNAs for *AaKr-h1* or *GFP* within 30 min after eclosion. At 96 h PE, fat bodies were dissected for total RNA extraction. The amount of individual transcripts in the dsKr-h1-injected and control mosquitoes was measured by quantitative RT-PCR. Data represent mean ± S.D. of three replicates. Statistical analysis was conducted using a paired t-test (*, $p<0.05$; **, $p<0.01$).

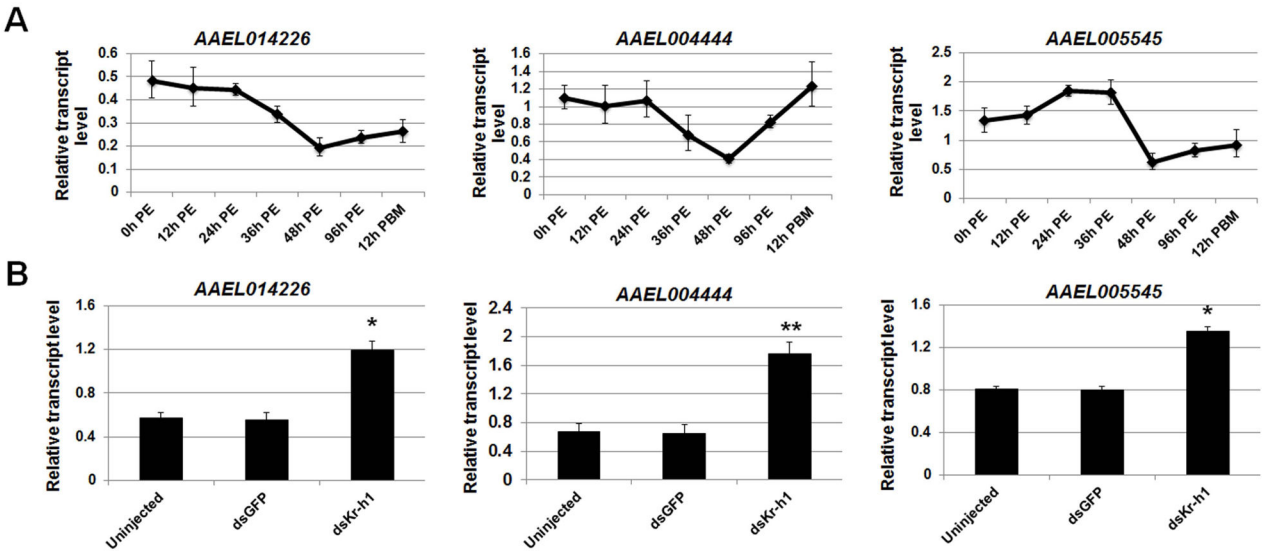

Figure 6.

AaKr-h1 acted as a repressor for the transcription of *AAEL014226*, *AAEL004444,* and *AAEL005545* in the previtellogenic mosquitoes. (*A*) Expression of the three AaKr-h1 target genes in the fat body of previtellogenic female mosquitoes. The amounts of specific mRNA were measured using real-time PCR. (*B*) RNAi-mediated depletion of AaKr-h1 increased the expression of *AAEL014226*, *AAEL004444* and *AAEL005545*. Newly emerged female mosquitoes were injected with dsRNAs for *AaKr-h1* or *GFP* within 30 min after eclosion. The amount of individual transcripts, in the dsKr-h1-injected and control mosquitoes at 96 h PE in the fat body, was measured by quantitative RT-PCR. Data represent mean ± S.D. of three replicates. Statistical analysis was conducted using a paired t-test (*, $p<0.05$; **, $p<0.01$).

Table 1

In vivo DNA binding sites of AaKr-h1 identified by ChIP-cloning

Locus of Cloned Fragment	Nearest Genes	Dist. (bp)	Gene Description
supercont1.1044:164199-164352	AAEL014226	5119	hypothetical protein
supercont1.107:238744-239418	AAEL004093	56658	hypothetical protein
supercont1.11:2072323-2073246	AAEL000580	51710	conserved hypothetical protein
supercont1.1131:133448-133780	AAEL014487	2510	conserved hypothetical protein
supercont1.119:81050-81549	AAEL004444	26464	conserved hypothetical protein
supercont1.122:2162654-2163511	AAEL004522	23305	gambicin anti-microbial peptide
supercont1.123:427346-427574	AAEL004556	18858	hypothetical protein
supercont1.15:19197-19725	AAEL000741	36598	ETS transcription factor E74
supercont1.15:4020480-4021282	AAEL000746	6893	NADP-specific isocitrate dehydrogenase
supercont1.162:628545-629795	AAEL005545	977	tetraspanin
supercont1.168:920752-920920	AAEL005651	3323	ethanolamine-phosphate cytidylyltransferase
supercont1.175:567643-568161	AAEL005822	15485	conserved hypothetical protein
supercont1.175:275807-276101	AAEL005810	47562	conserved hypothetical protein
supercont1.179:1278338-1278612	AAEL005904	45568	conserved hypothetical protein
supercont1.182:1219257-1220096	AAEL005957	10109	phospholipase b
supercont1.201:1048528-1049084	AAEL006330	22982	microtubule associated serine/threonine kinase
supercont1.204:795129-795831	AAEL006420	46740	conserved hypothetical protein
supercont1.21:600701-601222	AAEL001018	27084	conserved hypothetical protein
supercont1.221:351203-352060	AAEL006793	136	cytochrome P450
supercont1.248:1494624-1495531	AAEL007322	6253	phosphatidate phosphatase
supercont1.271:313573-314220	AAEL007652	1042	conserved hypothetical protein
supercont1.283:193494-193644	AAEL007814	1486	n-twist
supercont1.284:490057-490399	AAEL007817	4937	hypothetical protein
supercont1.297:121175-121372	AAEL017171	27830	
supercont1.383:1005986-1006368	AAEL009241	4645	translation initiation factor if-2
supercont1.454:393982-394164	AAEL017393	12268	
supercont1.50:2047109-2047800	AAEL002177	94868	serine-type enodpeptidase
supercont1.500:57637-58530	AAEL010717	12953	hypothetical protein
supercont1.536:203408-204079	AAEL018210	36784	
supercont1.545:535344-536084	AAEL011165	11899	conserved hypothetical protein
supercont1.55:1040026-1040168	AAEL002403	5724	hypothetical protein
supercont1.638:463831-463996	AAEL011959	37111	conserved hypothetical protein
supercont1.65:2535172-2536115	AAEL002705	93989	nucleolar protein c7b
supercont1.678:83033-83183	AAEL012319	25447	p20-CGGBP
supercont1.73:993813-993954	AAEL002949	16252	Osiris
supercont1.76:2041931-2042480	AAEL003050	16416	hypothetical protein
supercont1.76:62379-63323	AAEL003080	12694	hypothetical protein
supercont1.801:206028-206193	AAEL013177	9264	nucleotide-binding protein
supercont1.840:185133-186485	AAEL013415	28598	alpha-tropomyosin 5a